The Flow of Neutral Gas in the PFRC II

December 24, 2019: Kai Torrens

Abstract:

The inventory of hydrogen neutral gas within the PFRC-2 contributes to the ionization rate, axial and radial losses, momentum loss, current-drive efficiency, and plasma duration. We measure the neutral gas as a function of time using MKS capacitance manometers (baratrons) and ion gauges. The first are sensitive to pressure, the second to gas density. Both rapid (10 ms) and slow (1 s) response-time baratrons were placed on each of the PFRC-2's three vacuum chambers. The PFRC-2 center cell (CC) baratron saw a pressure rise at pulse initiation, consistent with the creation of Franck-Condon neutrals. That baratron also showed up to a 90% decrease in pressure maximizing 20 ms following each 3-10 ms RMF pulse. The pressure drop could be interpreted as ionization in the CC followed by axial transport of hydrogen ions out of the CC or implantation of the hydrogen into surfaces surrounding the plasma. The gauges outside the CC showed no concurrent pressure or density rise, mediating against the first interpretation. The pressure drop corresponds to an effective particle confinement time of 6 ms, consistent with recycling in the CC. Combined with theoretical calculations of gas conductance this experimental data allows us to construct a model for the equilibrium movement of neutral gas within the PFRC.

Introduction:

The Princeton Field Reversed Configuration (PFRC) device is currently being developed as a small, safe, and clean fusion power-source. These benefits rely on utilizing a high beta to fuse D-3He resulting in low neutron production and thus lower radiation and shielding requirements than other conventional fusion devices. This makes the PFRC especially promising as a candidate for mobile power supply or as a power source for spacecraft.

The successful development of the PFRC concept requires overcoming many challenges. The inventory of hydrogen neutral gas within the current iteration of the device, the PFRC-2, is integral to overcoming many of these challenges, as the behavior of neutral gas contributes to the ionization rate, axial and radial losses, momentum loss, current-drive efficiency, and plasma duration. In order to understand this behavior, we measure the neutral gas's pressure using MKS capacitive manometer, known as Baratrons. Two Baratrons were connected to each of the PFRC-2's three chambers: the source end cell (SEC), center cell (CC), and far end cell (FEC). One Baratron was connected almost directly to each chamber (fast Baratron) and one was connected via a long pipe and thus had a more delayed response rate (slow Baratron). Neutral gas is input in the SEC before diffusion into the CC and SEC. Both the CC and SEC are pumped down by turbo-pumps.

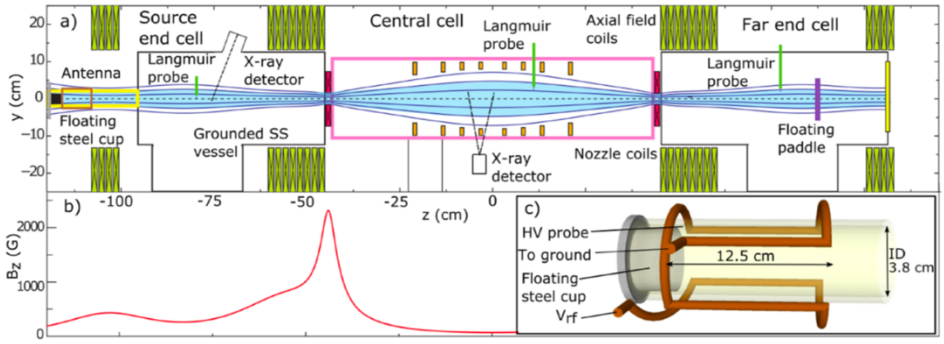

Fig 1: Diagram of the PFRC-2

In section 1 we present an explanation of our attempts to overcome noise limitations of our experimental setup; in section 2 we describe the basis of our theoretical time constants and conductances and present the results of our calculations; in section 3 we compare these values to the experimental data and attempt to reconcile the slight discrepancies we observe; in section 4 we present a simple model of equilibrium gas flow based on our time constants and conductances. In section 5 we emphasize important take aways from this work and the final section outlines profitable directions for future work based on our research.

Section 1: Noise Correction Methods and Their Limitations:

The PFRC relies on an odd parity rotating magnetic field (RMF_o) for current drive and heating, with a power ranging from 30-60 kW at present normal operating conditions. The RMF is typically applied in 3-50ms duration pulses, once per second. RMF generates a strong electromagnetic filed in the room and thus is a substantial source of background noise. The baratrons have probed especially susceptible to this noise and thus a noise correction method is necessary to get useful data about pressure changes during the RMF_o pulse. Two noise correction methods were explored: varying the length of the RMF pulse to reconstruct interim behavior, and taking and then subtracting a noise reading by closing the valves connecting the baratrons to the PFRC's chambers.

Subsection 1- Correction Method 1: Pulse Length Scan

While the baratron readings during the RMF_o pulse were unreliable due to noise pickup, the readings before the pulse were reliable and the baratron readings stabilized within roughly 10 ms after the pulse. This allowed us to calculate a reliable pressure drop over the entirety of the pulse. Shortening the pulse length allowed reconstruction of the pressure drop during longer pulses. That is, we assumed that the pressure drop during a 1ms RMF pulse was the same as the pressure drop 1ms into a 10ms RMF pulse of the same conditions. The following figure summarizes the results of this method.

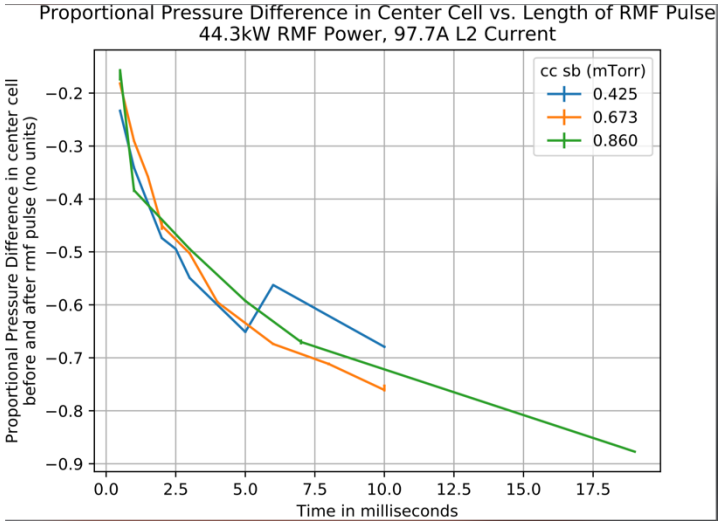

Fig 2: Each data point represents the average pressure drop during an RMF pulse of that length at the labelled starting pressure. Note the data at the lower fill pressures stops at 10ms discharges as the neutral gas pressure dropped too low to sustain further consistent plasma discharges when longer pulses were attempted.

As seen in fig 2 the pulse length scans revealed a consistent behavior over time at several different conditions, suggesting the pulse length scans illuminate a fundamental neutral gas dynamic. We speculate that the consistent proportion of the final pressure to the beginning pressure indicates plasma ionization that is consistently proportional to the inflow of gas and initial gas pressure. That is, a greater starting pressure and corresponding inflow of neutral gas led to plasma formation that ionized a proportionally larger amount of the gas. However, the idea that this data correctly represent the pressure drop during the RMF pulse rests on the assumption that the neutral gas behavior 1ms into a 10ms pulse is the same as the neutral gas behavior at the end of a 1ms pulse. This assumption is called into question by the results of the other correction method I explored. Thus, though intriguing these results remain speculative.

Subsection 2- Correction Method 2: Background Noise Readings and Subtraction

By closing the valves connecting the fast baratrons to each of the chambers, it was possible to take a reading of the RMF pickup experienced by a baratron at given conditions without confounding by meaningful pressure measurements. This noise measurement could then be subtracted from a given baratron's measurements at these same conditions. This correction consistently revealed a rise in pressure during the beginning of the RMF pulse followed by a sharp decrease in pressure (see fig 3) ultimately resulting in an overall pressure drop consistent with that seen by the RMF pulse length scans. The failure of the pulse length scan to reveal this initial pressure rise suggests it does not accurately represent the neutral gas's behavior during the RMF pulse. Thus, the background noise reading and subtraction method was the noise correction method employed for all the later measurements presented in this paper. However, it is important to identify two major limitations of this noise correction method.

Limitation 1: Potential Inconsistency

While we would expect fairly consistent interim pulse behavior at constant conditions, taking repeating pairs of noise corrections and measurements at the same conditions resulted in corrected data of varying consistency for different conditions.

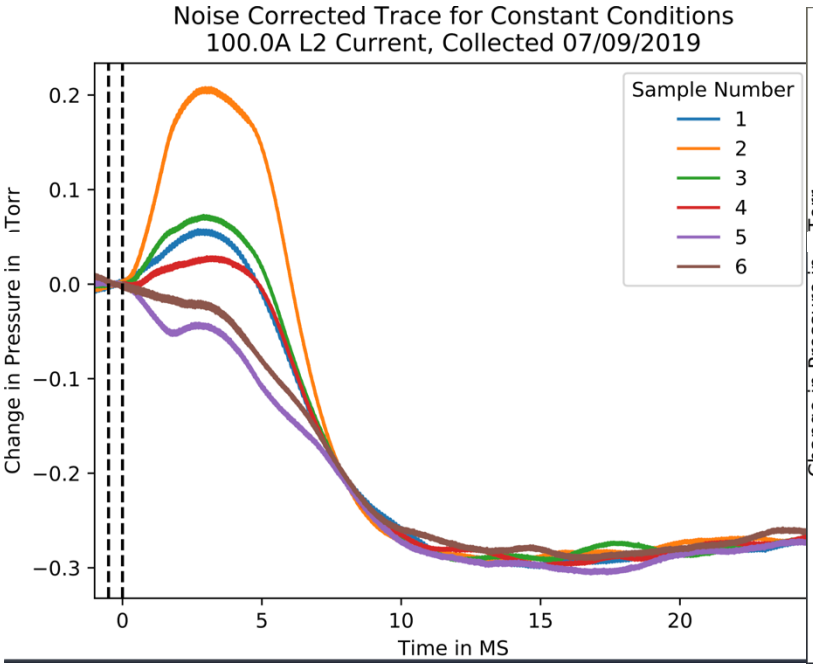

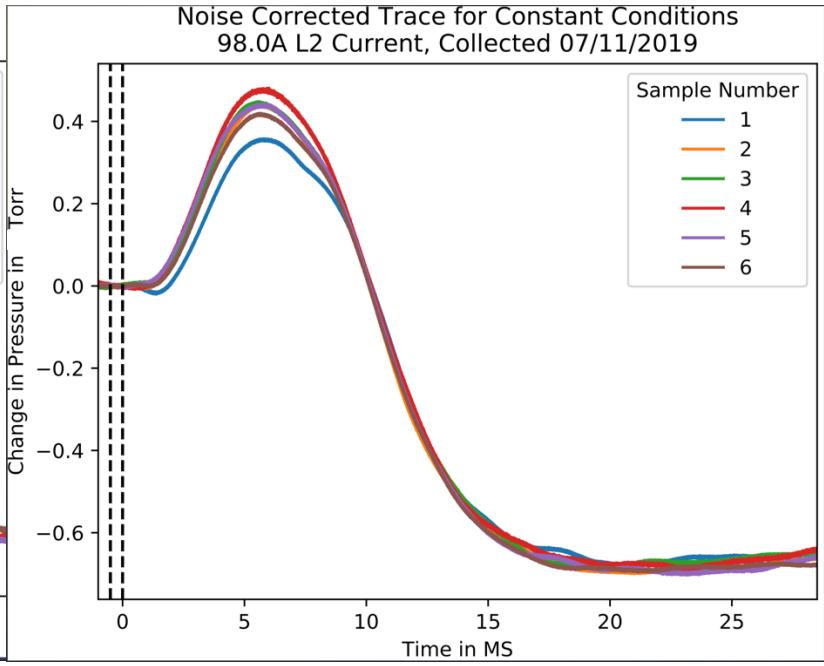

Fig 3: Repeated fast baratron corrections taken at around 400 mTorr (3a: left side) exhibit a greater variability of behavior than those taken at around 800 mTorr (3b: right side).

A closer look at the individual corrections used for each of the measurements in fig 3 reveals the corrected measurements on the left have far more inconsistent noise corrections than those on the right (see fig 4). This suggests that the background noise measurements are sometimes inconsistent.

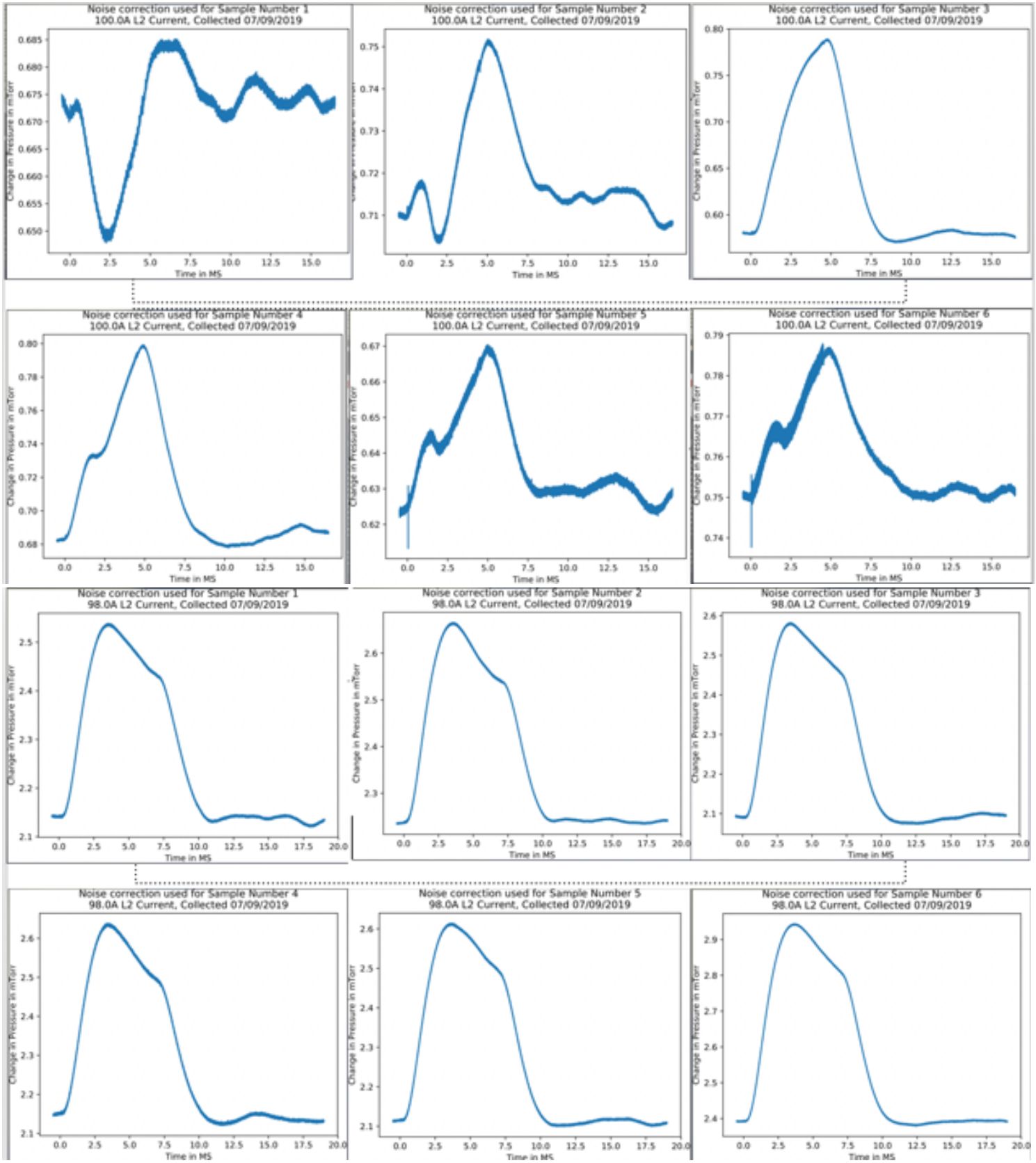

Fig 4: The top graphs show the fast baratron noise measurements used to produce fig 3a, while those on bottom show the fast baratron noise measurements used for fig 3b.

It is possible that this inconsistency in noise measurement is physically meaningful and is due to variable plasma behavior as plasma density measurements taken by the interferometer during this same period show much larger variability in plasma density for fig 3a than for fig 3b, but it could also simply reveal a weakness of this noise correction method.

Limitation 2: Mechanical Waves

Occasionally the noise correction measurements exhibit large scale oscillations. As these are not linked to any consistent starting conditions or plasma behavior we attribute them to mechanical noise. Using these corrections without first subtracting these oscillations does not clarify neutral gas behavior during the RMF pulse, but in fact further obscures it. This phenomenon will be visible in some of the data presented later in this paper.

Section 2- Theoretical Understanding of Gas Flow:

Gas flow is divided into three major categories based off the ratio of the molecular mean free path to the diameter of the piper known as the Knudsen number[1].

- Free Molecular flow: At high Knudsen numbers collisions with the pipe or chambers walls dominate the behavior of the gas
- Continuum flow: At low Knudsen numbers collisions with other gas particles dominate gas behavior.
- Transitional flow: At intermediate Knudsen numbers both forms of interactions are important for understanding gas behavior.

The neutral gas in the PFRC is at extremely low pressure, ……, and thus has a large molecular mean free path. We are thus confident that the neutral gas in the PFRC is best understood in the Free Molecular Flow continuum.

Subsection 1- Understanding Free Molecular Flow:

Free molecular flow has some parallels with electric circuits and we can think of a gas conductance (C) analogous to an electric conductance associated with each pipe or chamber the gas flows through. Thus, just as the overall behavior of a circuit can be inferred from the combined resistance of its components, the characteristic time it takes gas to flow between any chambers or sensors can be determined in terms of the conductances of the intervening components.

[1] *Flow of Gases Through Tubes and Orifices* by R. Gordon Livesey

Conductance Calculation Methods[2]:

The following method was used to calculate overall conductance for various components and groups of components. It is important to remember that conductance is zero dimensional and thus is only an approximation that may not be representative of complex geometries or larger volumes.

Overall Conductance: $C_m = C_a \alpha$ where C_a is the aperture conductance and α is the total transmission probability

$C_a = A\left(\sqrt{\frac{RT}{2\pi M}}\right)$

$\alpha = \frac{1}{1+\frac{3\cdot le}{8\cdot 3}}$ $\quad le = \left(1+\frac{1}{3+\frac{3\cdot l}{7\cdot R}}\right)\cdot l$ where l = length, R= radius

The inverse of the overall transmission probability α_t for a sequence of components can be calculated by adding the inverse of each components transmission probability and then subtracting an aperture correction scaled to the aperture area as summarized in the following equations.

$$\frac{1}{A_1}\left(\frac{1}{\alpha_{1n}}-1\right)=\sum_1^n\frac{1}{A_i}\left(\frac{1}{\alpha_i}-1\right)+\sum_1^{n-1}\left(\frac{1}{A_{i+1}}-\frac{1}{A_i}\right)\delta_{i,i+1}$$

with

$$\delta_{i,i+1}=1 \quad \text{for } A_{i+1}<A_i \text{ (reducing cross-sectional area)}$$

$$\delta_{i,i+1}=0 \quad \text{for } A_{i+1}\geq A_i \text{ (no reduction in cross-sectional area).}$$

Time Constants:

The characteristic time constant (T) is the time needed for the difference in pressure between two volumes to decrease to ~ 1/e of the original difference in pressure.

$T = V/C_m$ where V= volume of responding chamber
C_m=overall conductance between the two volumes

The total response time of a chamber to a change in pressure else ware is the time constant combined with the time it takes the H_2 to physically flow from one chamber to another. At T= 298 K H_2 has a velocity of 442 m/s or 40 cm/ms. The distance between chambers for most of the time constants presented are on the order of 40cm and so the additional time that should be added because of the finite speed of the H_2 gas is on the order of 1ms.

[2] The following equations and treatment are also credited to *Flow of Gases Through Tubes and Orifices* by R. Gordon Livesey

Table 1: Time Constants for Various Combinations of Components:

The two volumes	Time constant
CC to CC- Fast Baratron (CC-FB)	0.25 ms
Gas Puff to CC-FB	unclear as gas puff valve has a high pressure and may not be in molecular flow continuum
Gas Puff to whole CC Chamber	3.3x Gas Puff to CC-FB time constant
CC to FEC	0.55 s
CC to FEC-FB	0.25 ms
CC to SEC	0.78 s
CC to SEC-FB	~0.25 ms

Section 3- Theoretical Gas Flow Compared with Experimental Data:

The PFRC has a gas puff attached to its center cell. This allows us to input a small but consistent amount of gas at a known time and watch how the baratrons on all the chambers respond to the pressure change over time. We expected these response times to be on the order of time of the response time constants I had previously calculated if those response times are accurate.

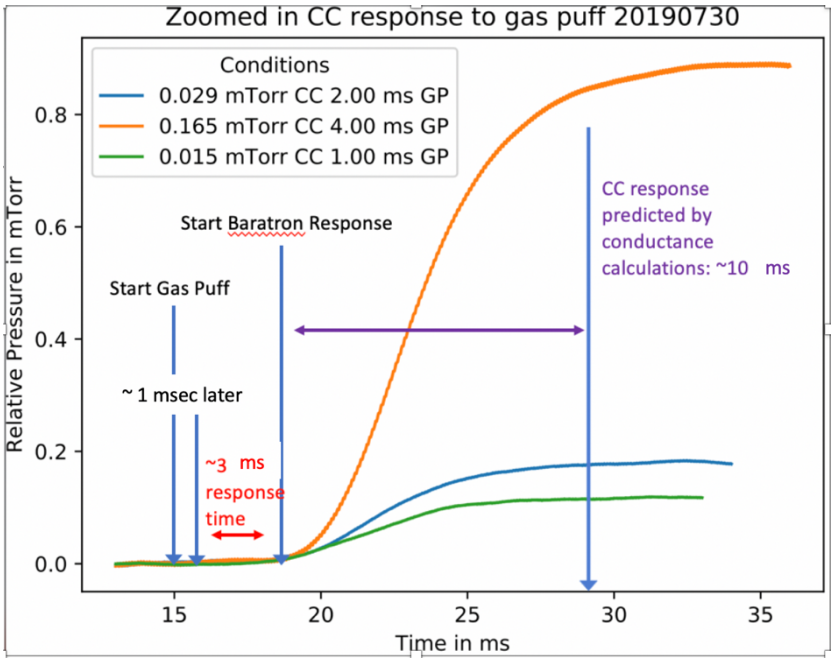

Fig 5: Short time response of the CC-FB to a gas puff at 15ms overlaid with the relevant predicted response time constant

The short time response of the CC-FB is a good match for what my response time constants predict. The one second delay accounts for the time needed for the H_2 to physically flow into the FB's response chamber. Thus, the characteristic time constant for the gas puff to CC-FB is ~3ms. From this I would predict a CC response time of roughly 10 ms. When lined up with the experimental data this correlates well with when the change in pressure the CC expresses starts to level off.

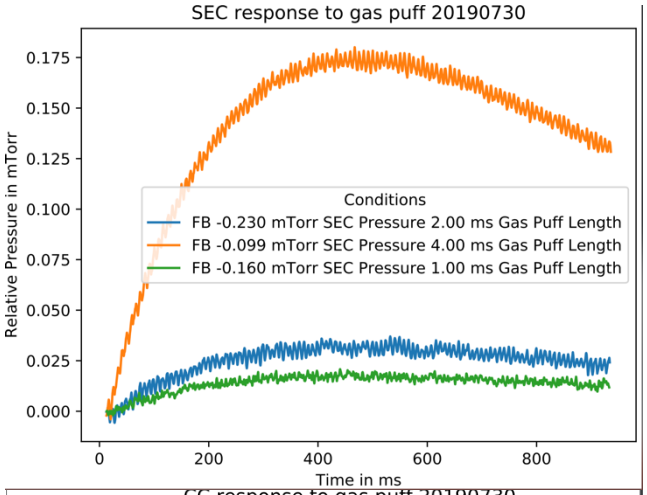

Fig 6 (top): Long time response of the SEC-FB to gas puff at 15ms. Theoretical Time Constant was 780 ms for the whole SEC chamber but the change in pressure the SEC expresses peaks around 450 ms

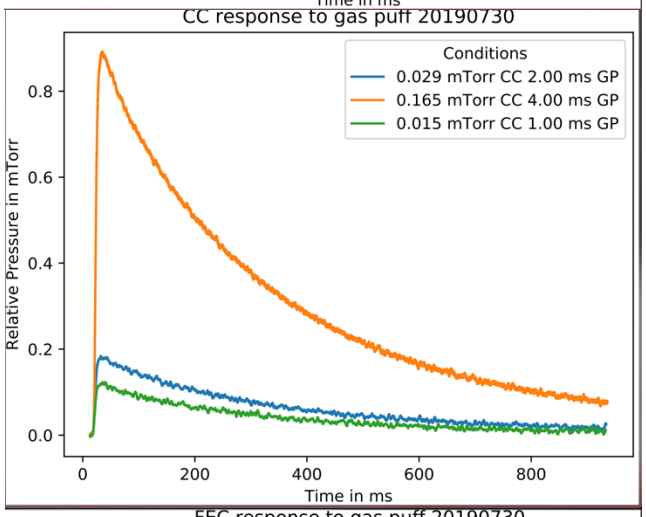

Fig 6 (middle): Long time view of the response of the CC-FB to gas puffs at 15 ms. The same data as shown in Fig 5. Note the exponential decay in pressure after the pulse

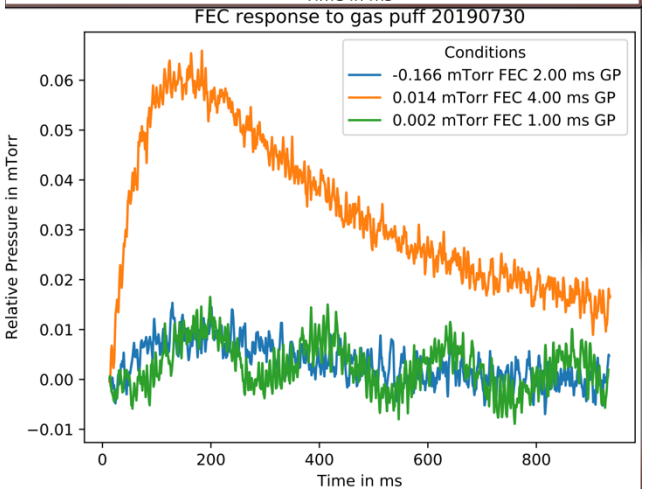

Fig 6 (bottom): Long time response of the FEC-FB to gas puff at 15ms. Theoretical Time Constant was 550 ms for the whole FEC chamber but the change in pressure the FEC expresses peaks around 200 ms. Large scale oscillations in 1 ms gass puff data (green) are due to large scale oscillations in the noise measurement obscuring the signal.

While the CC-FB short and long-time experimental data fit well with my theoretical calculations, the longtime response for both the SEC and FEC exhibit a markedly shorter time constant then predicted. Additionally, the ratio of response times is far different than expected. The 2 to 3 FEC time constant to SEC time constant ratio was predicted based off their 2 to 3 volume ratio and symmetric conductances, so the experimental ratio of 2 to 4.5 was unexpected.

One potential explanation for both the shorter response times and unexpected ratio is the action of the turbo pumps operating on both the CC and FEC. Since the gas puff is a small, one-time addition of gas, the action of these pumps may decrease the total amount of additional gas in the system before the SEC and FEC can come to equilibrium. By decreasing the equilibrium downwards towards the pressures the SEC and FEC had already reached, the maximum pressure in each chamber could be reached faster than the response time would suggest. Since the FEC has a turbo-pump acting directly on it, we would expect it to be more impacted by this potential effect and so to have a smaller relative time constant compared to the SEC. This correlates well with the smaller than expected 2 to 4.5 FEC to SEC time constant ratio we observed.

Section 4- One Dimensional Model of Gas Flow:

Conductance calculations can be used to construct a model of equilibrium gas flow through each chamber of the PFRC. When combined with the turbo pumps' pumping speeds and the pressure in any chamber of the PFRC, this model predicts expected equilibrium pressures in the other two chambers. These expected values can be compared with observed pressures when the RMF and plasma is being pulsed to identify when and how the plasma is having an effect on the neutral gas's behavior.

Corrected Pumping Speeds

The pumping rates of the turbo pumps connected to the CC and FEC are decreased by the conductance of the pipes connecting them to the chambers that they are pumping according to the following equation[3]:

$$\frac{1}{S_n} = \frac{1}{S} + \frac{1}{C_a}\left(\frac{1}{\alpha} - 1\right) = \frac{1}{S} + \frac{1}{C_m} - \frac{1}{C_a}.$$

Fig 7: Equation for calculating corrected pumping rate (S_n) based off pumping rate (S), aperture conductance (C_a), and transmission probability (α) or overall conductance (C_m).

[3] *Flow of Gases Through Tubes and Orifices* by R. Gordon Livesey

The turbo pump on the CC is a TV 141 Navigator ISO 100 with a pumping speed for H_2 of 100 l/s.[4] I calculated a corrected pumping speed of 74.6 l/s. The turbo pump on the FEC is a TV 551 Navigator CFF 6'' with a pumping speed for H_2 of 450 l/s.[5] I calculated a corrected pumping speed of 397 l/s.

Theoretical Equilibrium Model and Results

At equilibrium total gas flows into and out of all the chambers of the PFRC must be equal, as in the figure below. In addition, the rate of gas flow will not be changing at the equilibrium conditions.

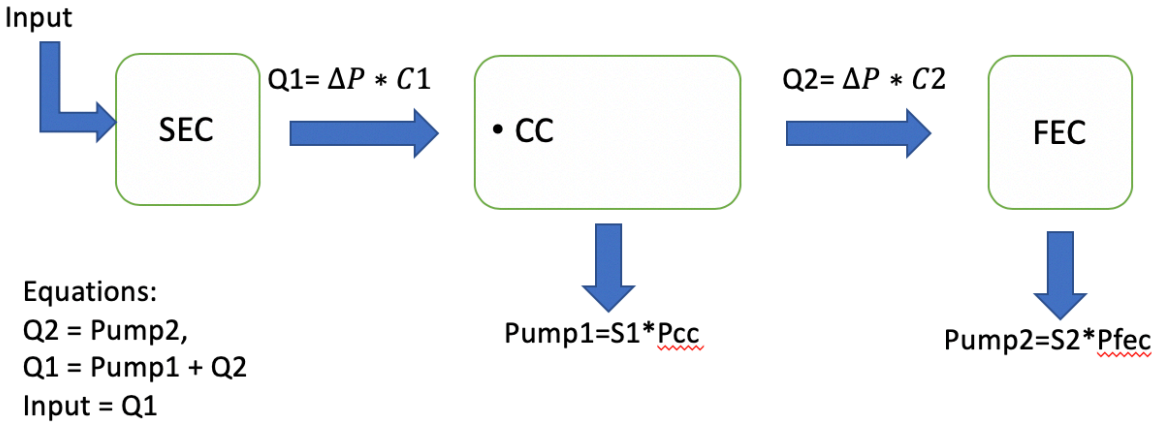

Fig 7: Diagram of equilibrium gas flow model. Q1= flow rate from SEC to CC, C1= Conductance from SEC to CC, Q2= flow rate from CC to FEC, C2= Conductance from CC to FEC, Pump1= flow rate out of CC, S1= corrected pumping rate of CC turbo, Pcc= pressure in CC, Pump2= flow rate out of FEC, S2= corrected pumping rate of FEC turbo, Pfec= pressure in FEC

I solved the equations resulting from these assumptions in terms of the pressure in the CC as this is the most experimentally reliable measurement. This resulted in an expected FEC pressure of 0.084*CC pressure and a SEC pressure of 3.98*CC pressure.

---

[4] *Description of the TV 141 Navigator* from Varian Vacuum Technologies http://www.ptb-sales.com/manuals/varian/tv141navrs485.pdf

[5] *TV 551/701 Navigator* from Agilent Technologies https://www.lesker.com/newweb/vacuum_pumps/pdf/manuals/tv551-701-navigator.pdf

Comparing the Model with Experimental Data

We ran gas through the PFRC in the absence of any RMF or plasma in order to provide real world equilibrium gas flow measurements to compare with my calculated equilibrium pressures. The ratios of FEC to CC and SEC to CC at a variety of CC pressures are displayed below.

Table 2: Experimental data compared to theoretical predictions

Pressure	Expected	0.1 mTorr	0.2 mTorr	0.3 mTorr	0.4 mTorr	0.5 mTorr	0.6 mTorr
Fec= xPcc	0.084	0.089	0.076	0.073	0.071	0.070	0.069
Sec= xPcc	3.98	2.73	2.45	2.53	2.58	2.54	2.56

As the table shows, the experimental data does not fit well with the predicted ratios of SEC to CC pressures. Next we present several potential explanations for this discrepancy as well as two potential corrections to the model, each of which, however, has associated problems.

Correction 1: New Conductances using Pumping Speeds

If we take our calculated pumping speeds as a given, we can use these and the experimental data to calculate corresponding conductances that should theoretically lead to such. These are displayed below.

Table 3: Original conductance compared to corrected conductance using different experimental conditions as basis for corrections.

Pressure	Expected	0.1 mTorr	0.2 mTorr	0.3 mTorr	0.4 mTorr	0.5 mTorr	0.6 mTorr
C1	36.185	120.8	113.7	111.8	110.8	110.2	109.8
C2	36.185	38.9	32.9	31.3	30.5	30.0	29.6

However, as mentioned in the section on gas puff experimental data, the connections between the SEC and CC and the FEC and CC are believed to be symmetric, thus the we would expect the

conductances (C1 and C2) to be the identical. This strongly suggests that the pumping speeds are different then as given or that the data captures behavior beyond the theoretical model.

Correction 2: New Pumping Speeds using Conductances

Similarly to correction 1, if we take the conductances as given, we can use these and the experimental data to calculate corresponding pumping speeds displayed below.

Table 4: Original pumping speeds compared to corrected speeds using different experimental conditions as basis for corrections

Pressure	Expected	0.1 mTorr	0.2 mTorr	0.3 mTorr	0.4 mTorr	0.5 mTorr	0.6 mTorr
S1 (l/s)	397.266	369.9	437.4	460.4	472.1	480.1	485.8
S2 (l/s)	74.64	24.1	16.3	20.1	22.0	21.0	21.9

However, some of the corrected pumping speed for the turbo pump connected to the FEC (S1) exceed the maximum pumping speed given by the manufacturer (450 l/s). Since the pipes connecting the pump to the FEC chamber will only decrease the pumping speed. This strongly suggests either the conductances are different then as given or that the data captures behavior beyond the theoretical model.

Other Explanations

The results of the previous correction methods suggest one of three things: Firstly, some combination of the corrections could be correct. For example, that there is a previously unregarded slight asymmetry in the connections between the FEC and CC and between the SEC and CC combined with a higher S1 and lower S2 then I calculated.

Secondly, the pressure data could be inaccurate. Most straightforwardly, the data at various pressures in the CC displays a fair amount of variability, so the inconsistencies could be due to random variability. More subtly, the SEC came from a slow baratron (SB) and an ion gauge (IG). Due to a malfunction, this SB is unable to be zeroed. We estimated the zero by fitting a line to the experimental data and subtracting the y intercept, but this correction may not have been adequate. Additionally, the SEC-IG was operating near its upper pressure limit during this data collection and displayed a non-linear response compared to the highly reliable CC-SB, calling its data into question as well.

Finally, the experimental data's incompatibility with my theoretical model could also be evidence of some mistake in the theoretical model, either computational, or some oversimplification or misunderstanding of the nature of gas flow in the PFRC.

Section 5- Conclusion:

Understanding the flow of neutral gas in the PFRC-2 is crucial to the successful development of the device as a fusion power device. This paper presented two possible noise correction methods to help extract accurate experimental pressure data from the noisy baratron data. Free Molecular Flow and conductance were explored as a theoretical basis for understanding gas flow in the PFRC-2. The predictions of this theoretical basis were compared with experimental data and a potential explanation for inconsistencies between the two was presented. Finally, this theoretical grounding was used to create a simple model to predict equilibrium pressure of gas in the PFRC-2. Several explanations for the inconsistency of this model were presented. Critically, a full particle inventory of the PFRC-2 remains elusive as much of the neutral gas remains unaccounted for after ionization. The pressure drop in each of the cells corresponds to ionizing gas, but we would expect these ions to eventually reform neutral particles and thus there to be a corresponding increase in pressure at some point. However, we never observe this. The lack of increase in pressure cannot be explained through changes in the background rate of gas flow into and out of the machine, as decreased pressure in the SEC should correspond to a greater rate of inflowing gas and a lower pressure in the FEC should correspond to a lesser rate of gas outflow, not the opposite. While the exact amount of missing gas varies based on starting conditions to give a sense of the magnitude of missing gas we estimate the amount of missing gas for 5mTorr by comparing starting pressure and the pressure 20 ms after the pulse and finding the corresponding loss of particles (I estimate that over this short time interval the amount of gas removed by the turbo pumps is roughly equivalent to that coming in from gas inflow). This calculation results in an estimate of 8.6*(10^-4) moles of missing gas. This thus remains a very important avenue of future inquiry.

Section 6- Opportunities for Future Work:

Clarifying Corrections to the Theoretical Model:

Further experimental data points at lower and higher CC pressures would help clarify the reliability of the SEC-SB zeroing method and the SEC-IG data's reliability. Additionally, they could help to decrease overall variability. Finally, they could provide insight into how to best correct my theoretical model as their data points may be more consistent with one correction method than with another. Rechecking the relevant conductances and corrected pumping speeds could also help to illuminate which, if either, correction method is more correct.

Extending the Theoretical Model:

Conductance ability to predict the flow rate of gas can be used not only to calculate equilibrium pressures but also expected changes in pressure based on that gas flow. In other

words, it provides not only expected pressures but also expected pressure derivatives. This ability could be added to my model to further illuminate where the neutral gas is not behaving as expected, and thus where plasma effects are occurring.

Particle Inventory:

The most important avenue for further work, as mentioned in the conclusion, is continued work toward a full particle inventory. Further work understanding the behavior of neutral gas will be helpful toward this end, but better accounting of electron and ion behavior will also be crucial. Achieving this accounting in tandem would allow each to serve as a way to check the others. Finally, as surface implantation of hydrogen seems a likely avenue for the gas to go missing, studying the plasma-surface interactions in the PFRC-II would prove very fruitful in this effort as well.

Acknowledgments:

I would like to thank Eugene Evans and Dr. Samuel Cohen for their incredible insight, patience, and overall support this summer. I would also like to thank the whole lab team for their guidance and for numerous helpful conversations. Finally, I would like to thank the other summer interns.

This work was funded by Princeton Environmental Institute (PEI)

References

Flow of Gases Through Tubes and Orifices by R. Gordon Livesey

Description of the TV 141 Navigator from Varian Vacuum Technologies http://www.ptb-sales.com/manuals/varian/tv141navrs485.pdf

TV 551/701 Navigator from Agilent Technologies https://www.lesker.com/newweb/vacuum_pumps/pdf/manuals/tv551-701-navigator.pdf